

Madden-Julian Oscillation: Recent Evolution, Current Status and Predictions



Update prepared by:
Climate Prediction Center / NCEP
31 August 2015

Outline

Overview

Recent Evolution and Current Conditions

MJO Index Information

MJO Index Forecasts

MJO Composites

Overview

The MJO remained weak during the past week.

Other types of variability, including the ongoing El Niño and tropical cyclone activity over the Pacific basin, remain the primary drivers of the global tropical convective pattern.

Dynamical models continue to be highly divergent due to the incoherent intraseasonal pattern, with most depicting little MJO signal over the next two weeks.

The MJO is not expected to play a role in the pattern of tropical convection during the next two weeks. The low frequency ENSO state and other types of tropical variability, such as tropical cyclones, are expected to have more influence.

Additional potential impacts across the global tropics and a discussion for the U.S. are available at:
<http://www.cpc.ncep.noaa.gov/products/precip/CWlink/ghazards/index.php>

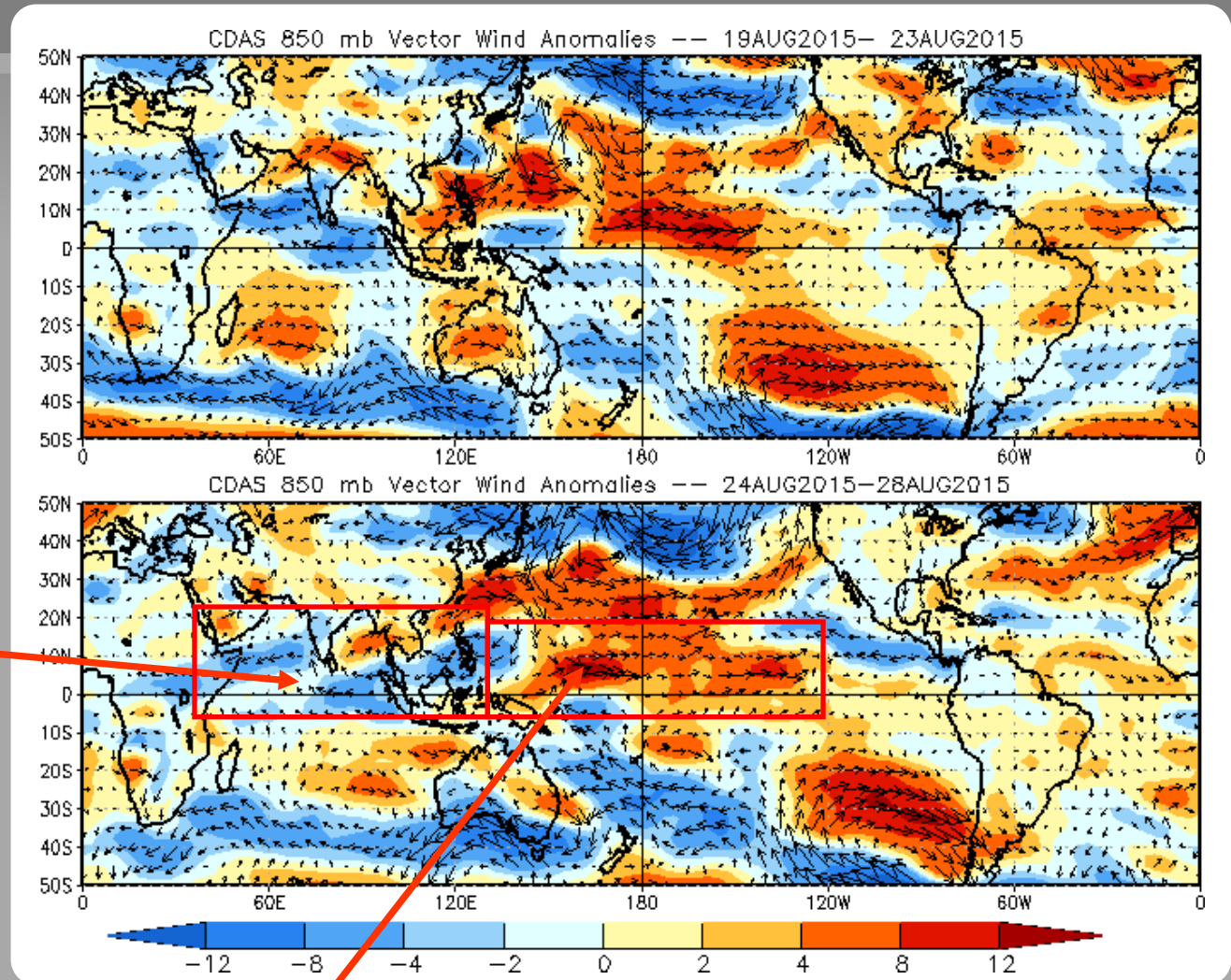
850-hPa Vector Wind Anomalies (m s^{-1})

Note that shading denotes the zonal wind anomaly

Blue shades: Easterly anomalies

Red shades: Westerly anomalies

Easterly anomalies persisted over parts of South Asia, the northern Indian Ocean, and the western Maritime Continent.



Strong westerly wind anomalies persisted over the central north Pacific, partly due to ongoing tropical cyclone activity.

850-hPa Zonal Wind Anomalies (m s⁻¹)

Westerly anomalies (orange/red shading) represent anomalous west-to-east flow

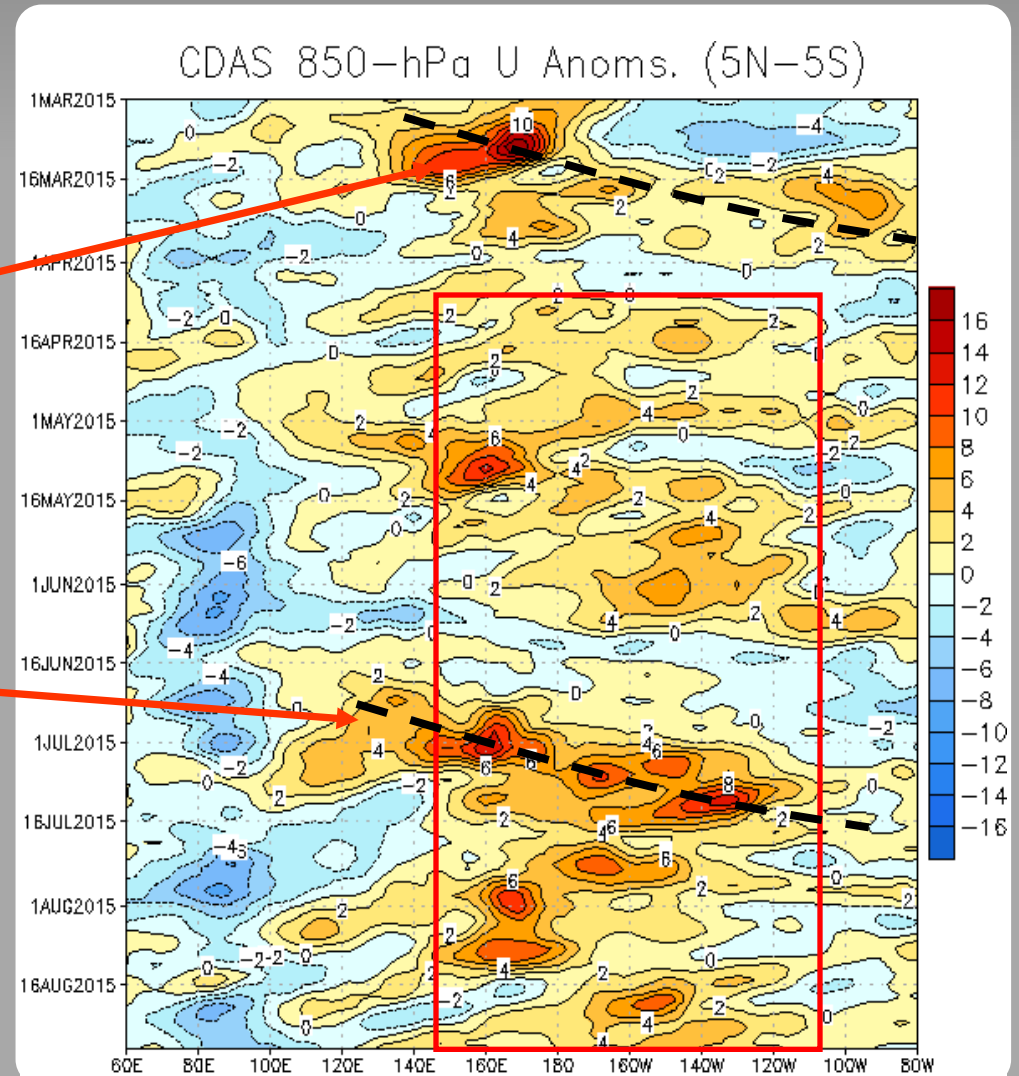
Easterly anomalies (blue shading) represent anomalous east-to-west flow

The MJO, Rossby wave activity, and El Niño conditions contributed to a strong westerly wind burst in early March.

The red box highlights the persistent low-frequency westerly wind anomalies associated with ENSO. Some transient variability is observed as well.

A robust MJO event was observed in late June through mid-July, constructively interfering with the background state.

Recently, the background ENSO remains the primary signal, but other modes, including tropical cyclone activity near and east of the Date Line, continue to influence the pattern.



OLR Anomalies - Past 30 days

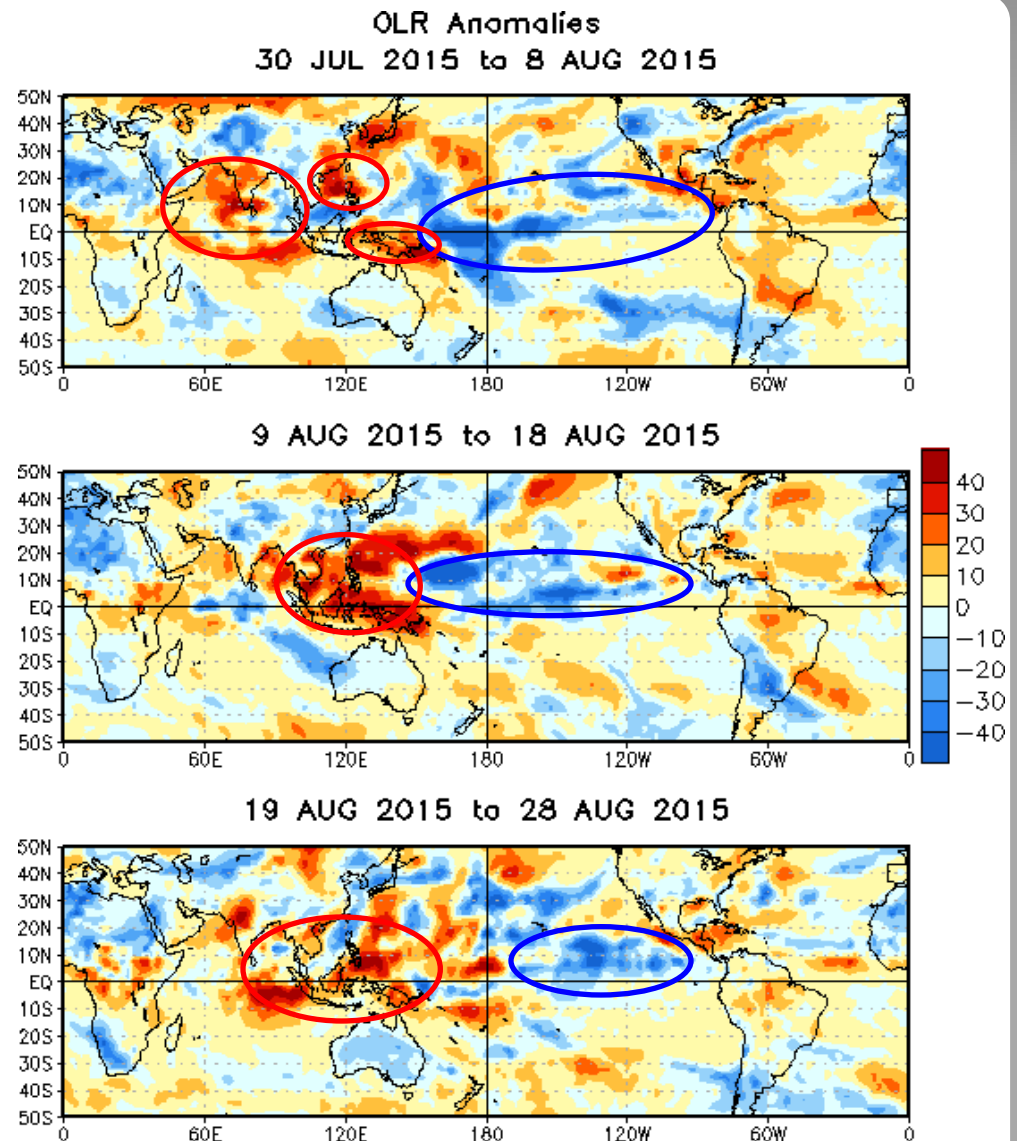
Drier-than-normal conditions, positive OLR anomalies (yellow/red shading)

Wetter-than-normal conditions, negative OLR anomalies (blue shading)

During early August, the ENSO signal remained prominent, with generally suppressed (enhanced) convection over the Indian Ocean and parts of the Maritime Continent (central and eastern Pacific).

The suppressed signal intensified over the Maritime Continent during mid-August, while enhanced convection persisted across the Pacific.

During late August, the large-scale pattern remained relatively unchanged, with suppressed (enhanced) convection over the Maritime Continent (eastern Pacific). Tropical cyclone activity both west and east of Hawaii was evident in the OLR field.



Outgoing Longwave Radiation (OLR) Anomalies (2.5°N-17.5°N)

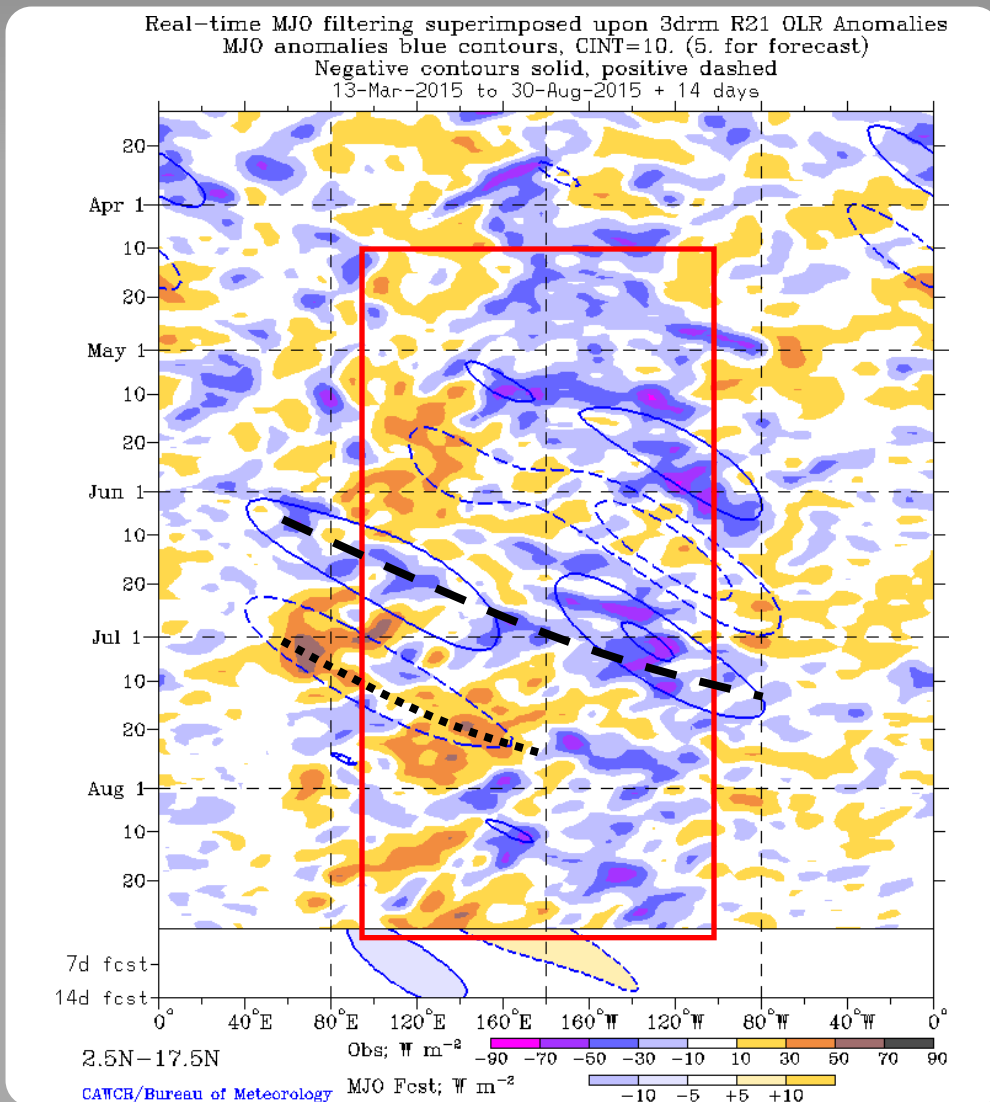
Drier-than-normal conditions, positive OLR anomalies (yellow/red shading)

Wetter-than-normal conditions, negative OLR anomalies (blue shading)

Since April, the ongoing El Niño is observed (red box) as a tendency toward a dipole of anomalous convection extending from the Maritime Continent (suppressed) to the East Pacific (enhanced).

During June and early July, the MJO become active, interfering with the ENSO signal at times.

Recently, the MJO signal has weakened and other types of tropical variability, including El Niño and tropical cyclones, are more influential.



200-hPa Velocity Potential Anomalies (5°S - 5°N)

Positive anomalies (brown shading) indicate unfavorable conditions for precipitation

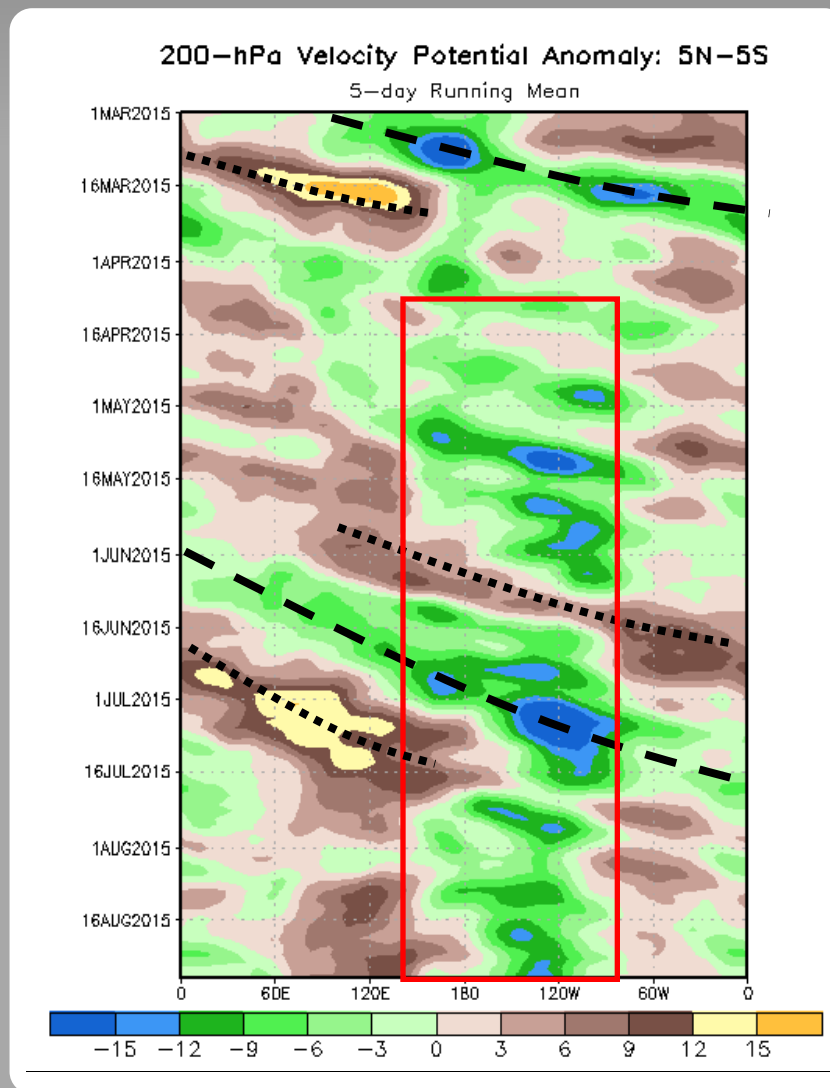
Negative anomalies (green shading) indicate favorable conditions for precipitation

The MJO strengthened in early March as seen in the upper-level velocity potential anomalies.

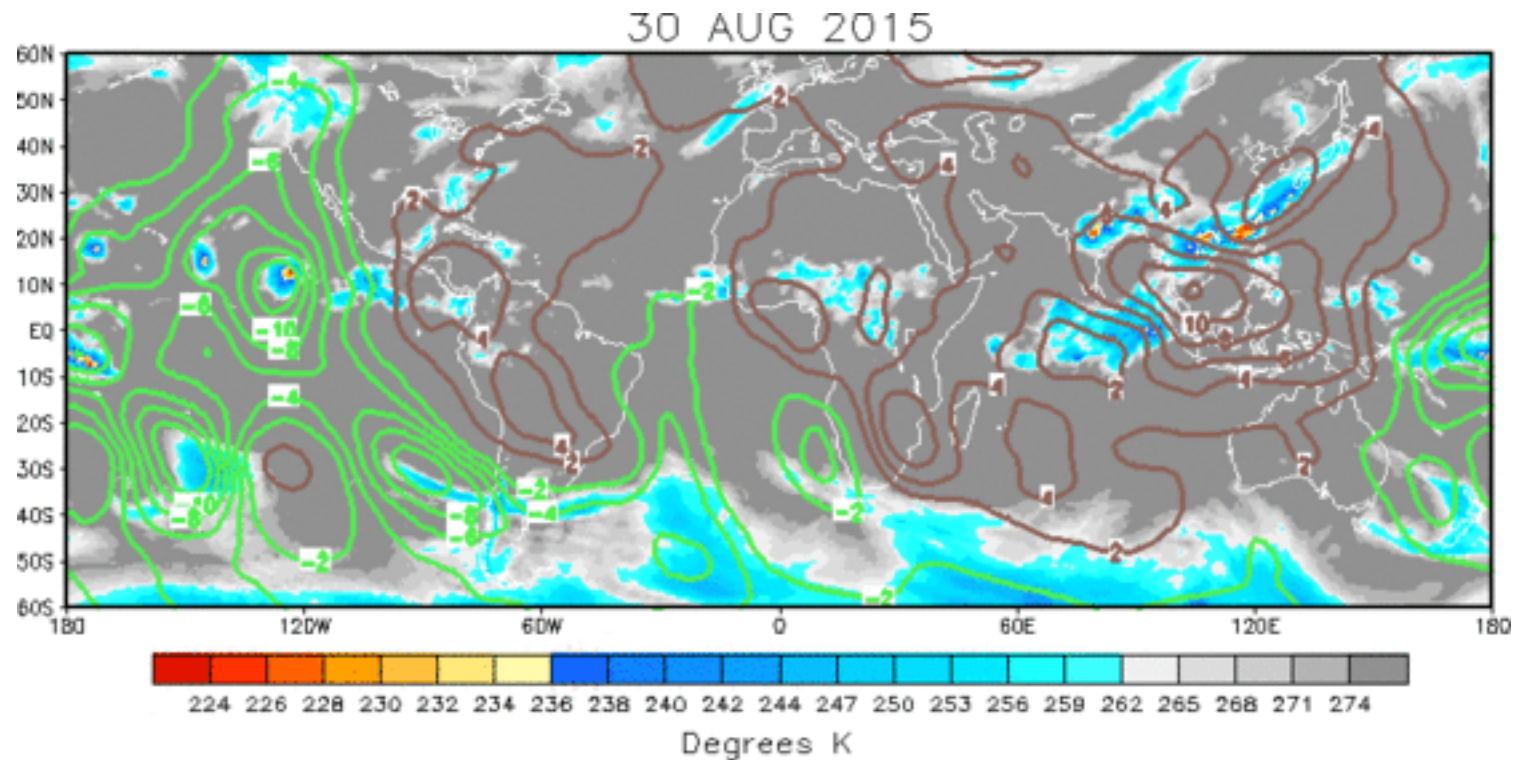
The developing ENSO state is highlighted by the red box, showing anomalous divergence over the central and eastern Pacific. This pattern has only been temporarily interrupted by strong Kelvin wave/MJO activity at times.

During June and early July, a high-amplitude MJO event was observed, constructively interfering with the El Niño signal in early July. By the end of July, the MJO weakened as the low-frequency state dominated the pattern of tropical variability.

More recently, a generally stationary pattern reflective of El Niño conditions was observed.



IR Temperatures (K) / 200-hPa Velocity Potential Anomalies



The upper-level velocity potential pattern continues to show anomalous upper-level divergence over the central and eastern Pacific with upper-level convergence over the Indian Ocean and the Maritime Continent.

Positive anomalies (brown contours) indicate unfavorable conditions for precipitation
Negative anomalies (green contours) indicate favorable conditions for precipitation

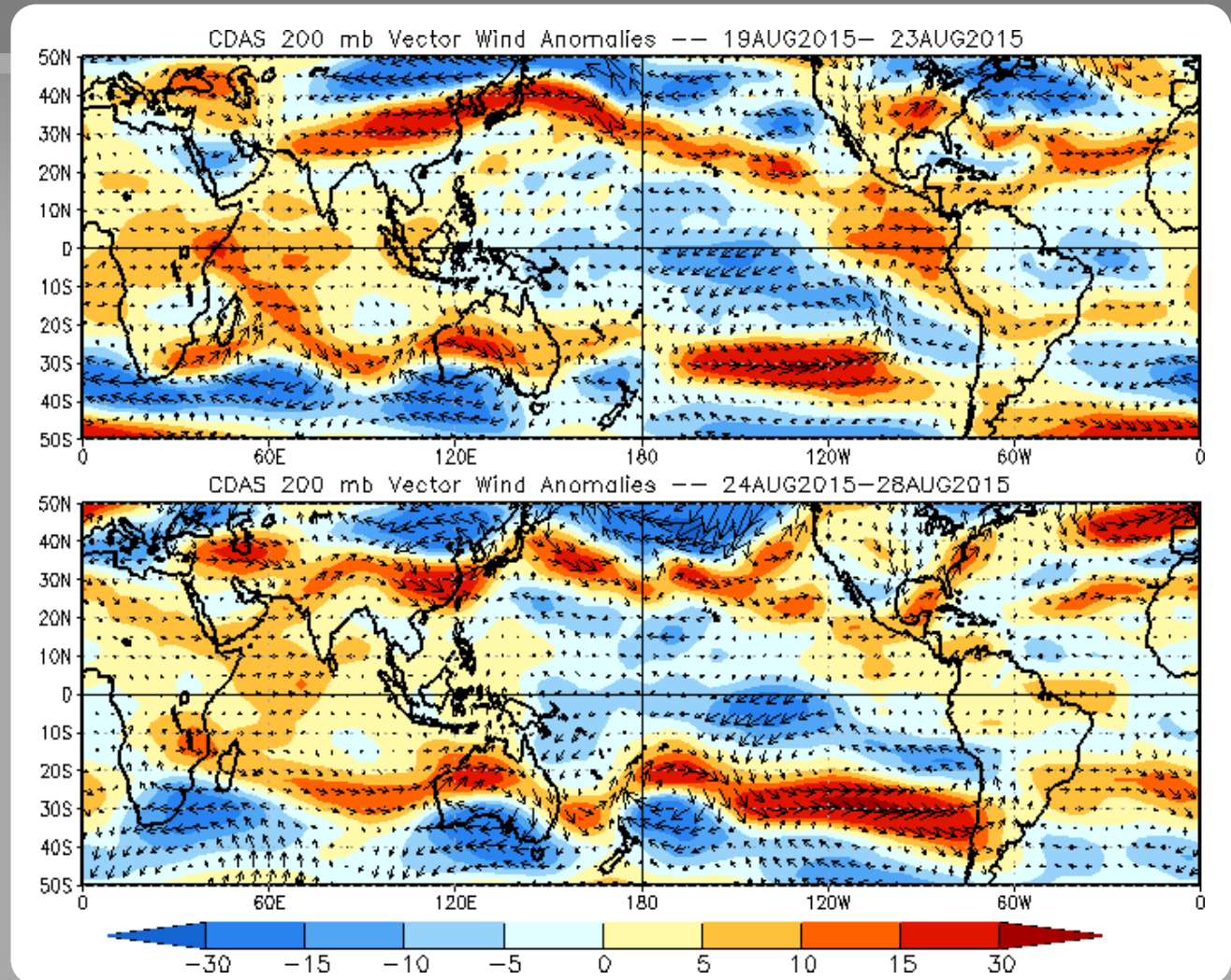
200-hPa Vector Wind Anomalies (m s^{-1})

Note that shading denotes the zonal wind anomaly

Blue shades: Easterly anomalies

Red shades: Westerly anomalies

Westerly anomalies weakened somewhat over the far eastern Pacific.



200-hPa Zonal Wind Anomalies (m s⁻¹)

Westerly anomalies (orange/red shading)
represent anomalous west-to-east flow

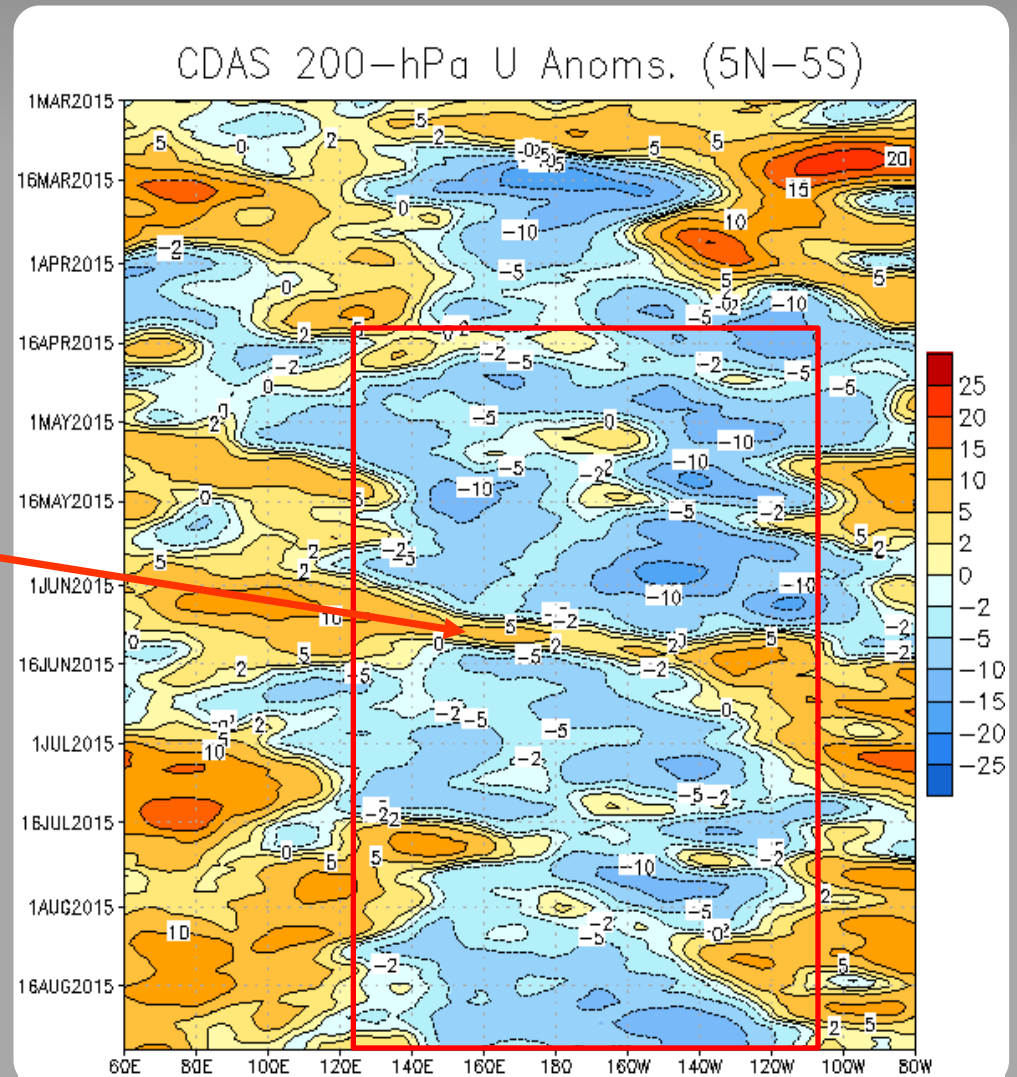
Easterly anomalies (blue shading) represent
anomalous east-to-west flow

Easterly anomalies have persisted over the
central and eastern Pacific associated with El
Niño since mid-April (red box).

During June, these easterly anomalies were
interrupted by robust atmospheric Kelvin
wave/MJO activity.

During August, some westward propagation
of westerly anomalies from the Maritime
Continent to the Indian Ocean was evident.

Recently, easterly anomalies strengthened
over the eastern Pacific.



Weekly Heat Content Evolution in the Equatorial Pacific

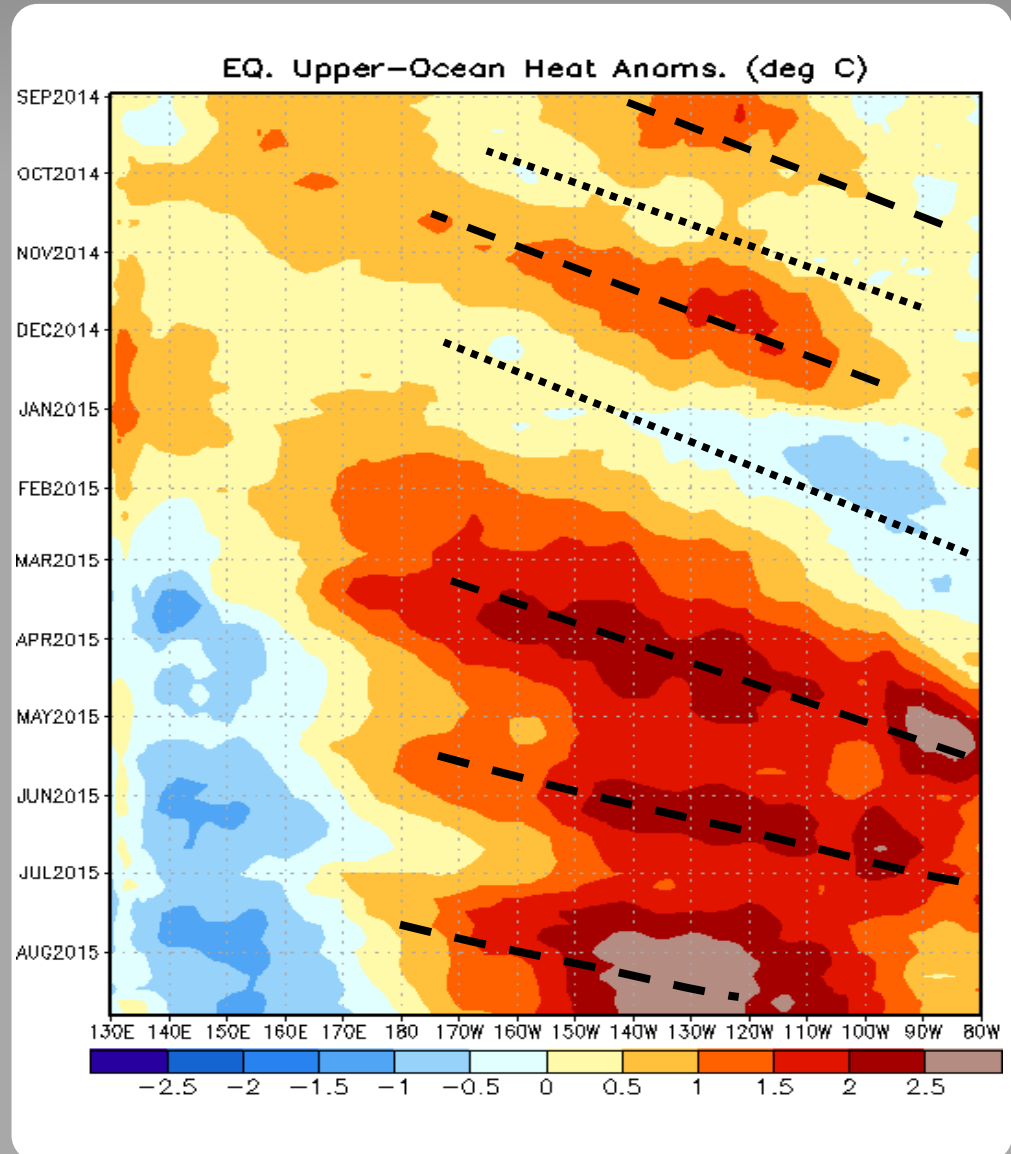
Oceanic Kelvin waves have alternating warm and cold phases. The warm phase is indicated by dashed lines. Downwelling and warming occur in the leading portion of a Kelvin wave, and upwelling and cooling occur in the trailing portion.

During October-November, positive subsurface temperature anomalies increased and shifted eastward in association with the downwelling phase of a Kelvin wave. During November - January, the upwelling phase of a Kelvin wave shifted eastward.

Following a strong westerly wind burst in March, another downwelling phase of a Kelvin wave propagated eastward, reaching the South American coast during May.

Reinforcing downwelling events have followed, resulting in persistently above-normal heat content from the Date Line to 90W.

Heat content anomalies greater than 2.5°C were observed over the east-central Pacific with the latest oceanic Kelvin Wave.



MJO Index -- Information

The MJO index illustrated on the next several slides is the CPC version of the Wheeler and Hendon index (2004, hereafter WH2004).

Wheeler M. and H. Hendon, 2004: An All-Season Real-Time Multivariate MJO Index: Development of an Index for Monitoring and Prediction, *Monthly Weather Review*, 132, 1917-1932.

The methodology is very similar to that described in WH2004 but does not include the linear removal of ENSO variability associated with a sea surface temperature index. The methodology is consistent with that outlined by the U.S. CLIVAR MJO Working Group.

Gottschalck et al. 2010: A Framework for Assessing Operational Madden-Julian Oscillation Forecasts: A CLIVAR MJO Working Group Project, *Bull. Amer. Met. Soc.*, 91, 1247-1258.

The index is based on a combined Empirical Orthogonal Function (EOF) analysis using fields of near-equatorially-averaged 850-hPa and 200-hPa zonal wind and outgoing longwave radiation (OLR).

MJO Index - Recent Evolution

The axes (RMM1 and RMM2) represent daily values of the principal components from the two leading modes

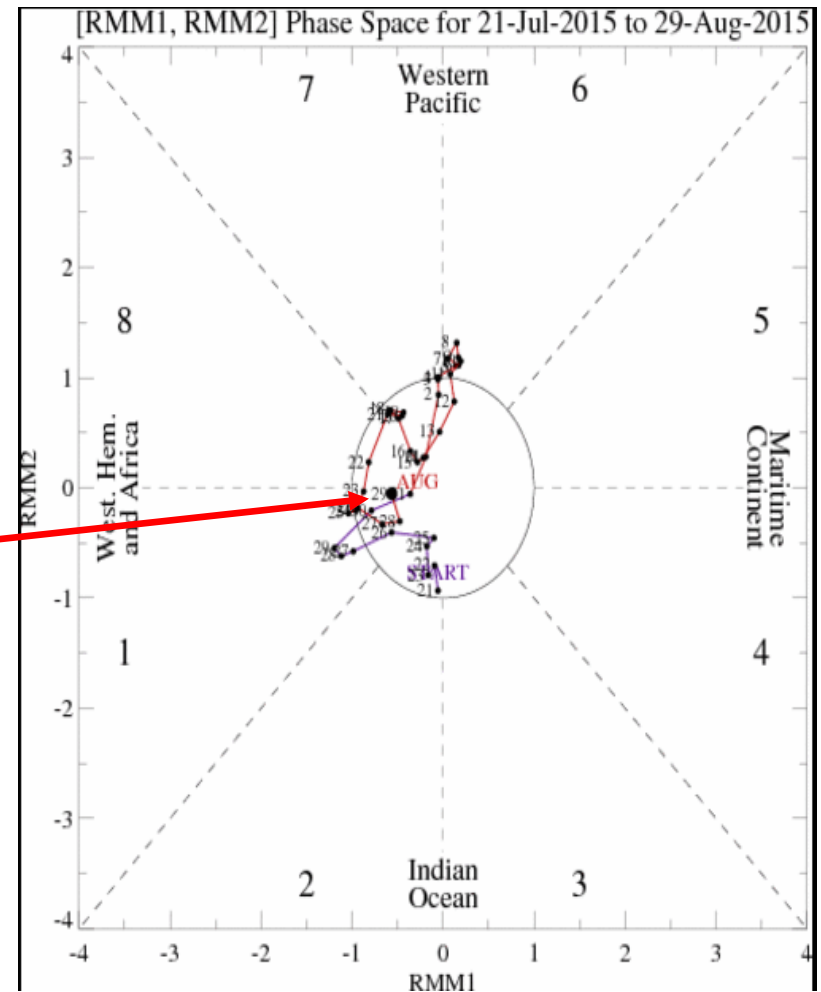
The triangular areas indicate the location of the enhanced phase of the MJO

Counter-clockwise motion is indicative of eastward propagation. Large dot most recent observation.

Distance from the origin is proportional to MJO strength

Line colors distinguish different months

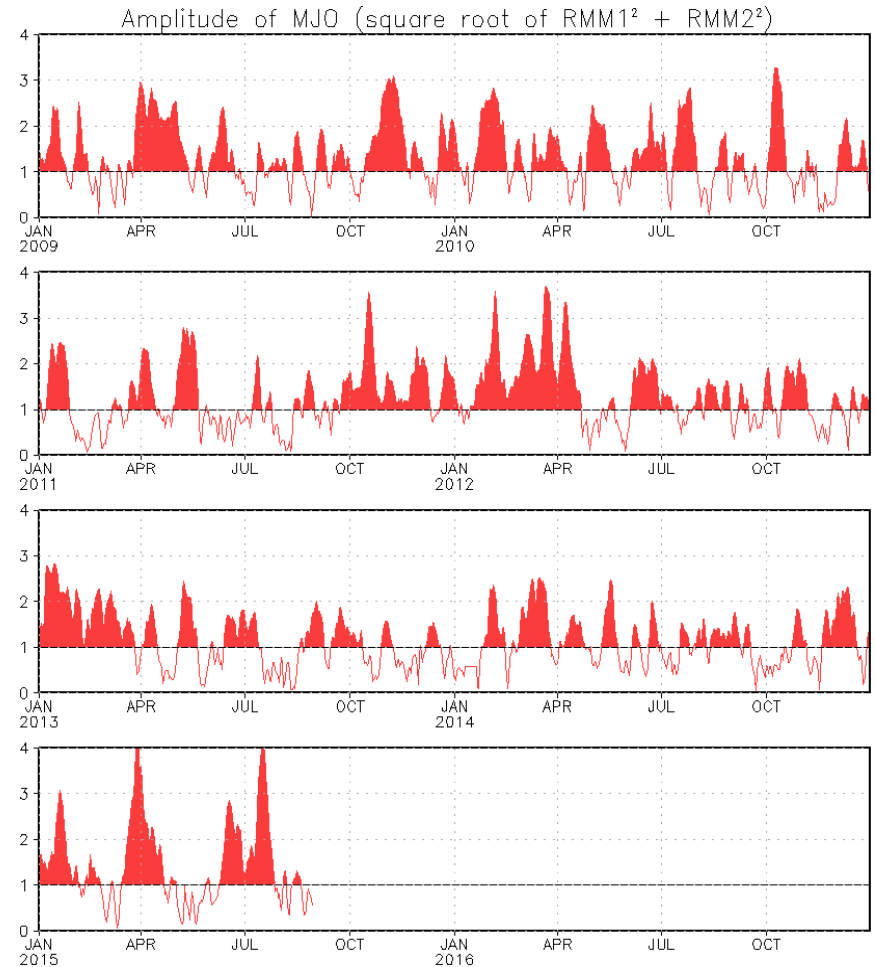
The MJO index indicated weak MJO activity during the past few weeks.



MJO Index - Historical Daily Time Series

Time series of daily MJO index amplitude for the last few years.

Plot puts current MJO activity in recent historical context.



Ensemble GFS (GEFS) MJO Forecast

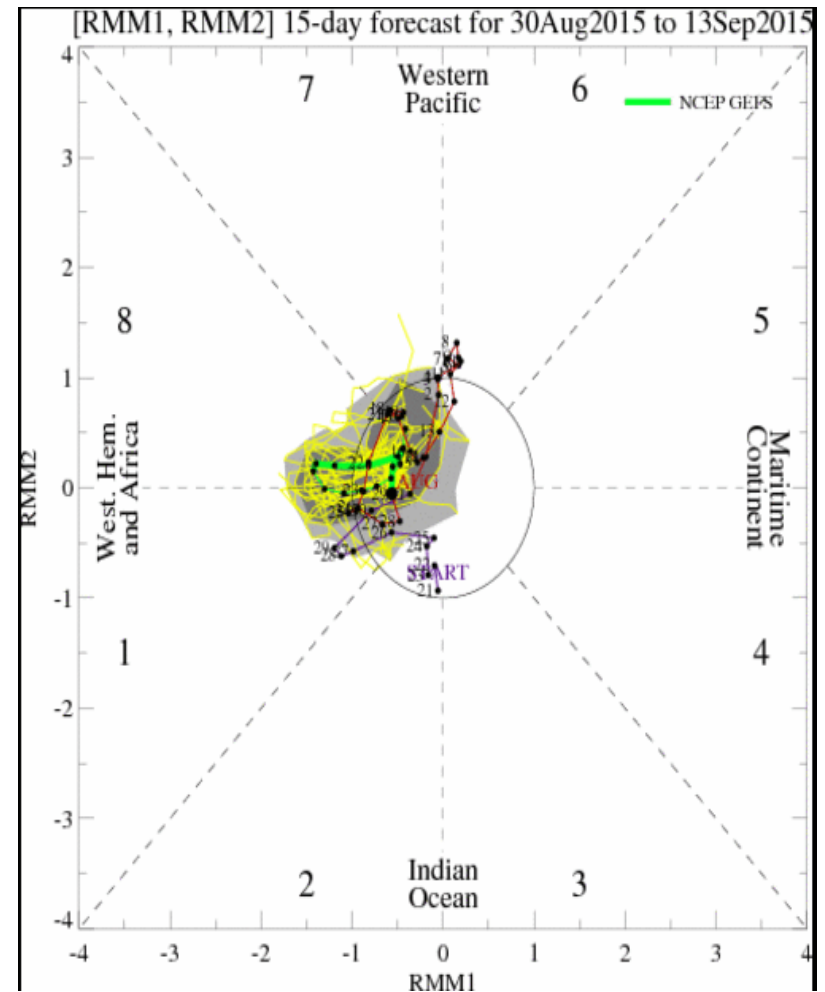
RMM1 and RMM2 values for the most recent 40 days and forecasts from the ensemble Global Forecast System (GEFS) for the next 15 days

light gray shading: 90% of forecasts

dark gray shading: 50% of forecasts

The GFS ensemble MJO index forecast depicts no coherent MJO signal during the next two weeks.

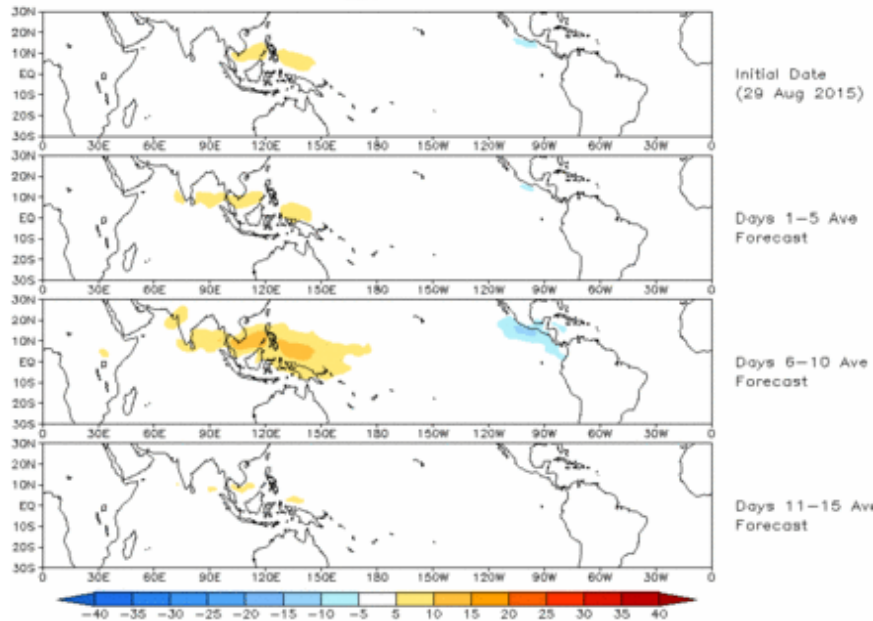
Yellow Lines - 20 Individual Members
Green Line - Ensemble Mean



Ensemble GFS (GEFS) MJO Forecast

Spatial map of OLR anomalies for the next 15 days

Prediction of MJO-related anomalies using GEFS operational forecast
Initial date: 29 Aug 2015
OLR

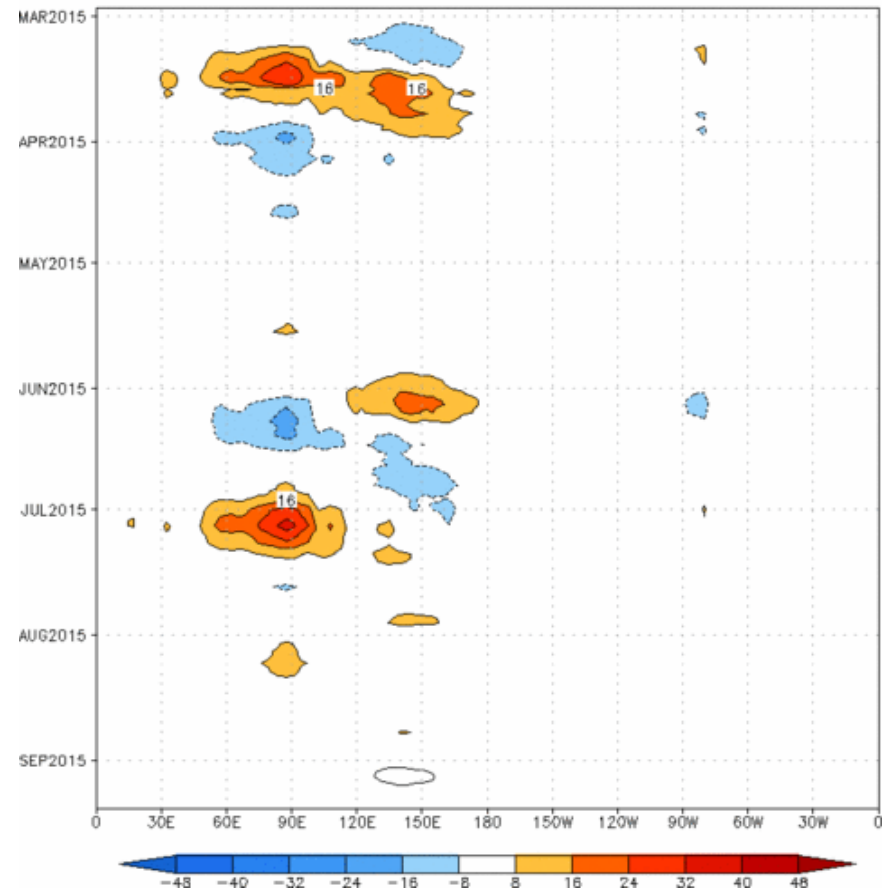


The GEFS MJO index-based OLR forecast depicts a weak anomaly pattern during the next two weeks, consistent with the weak MJO index forecasts.

Figures below show MJO associated OLR anomalies only (reconstructed from RMM1 and RMM2) and do not include contributions from other modes (*i.e.*, ENSO, monsoons, etc.)

Time-longitude section of (7.5° S-7.5° N) OLR anomalies - last 180 days and for the next 15 days

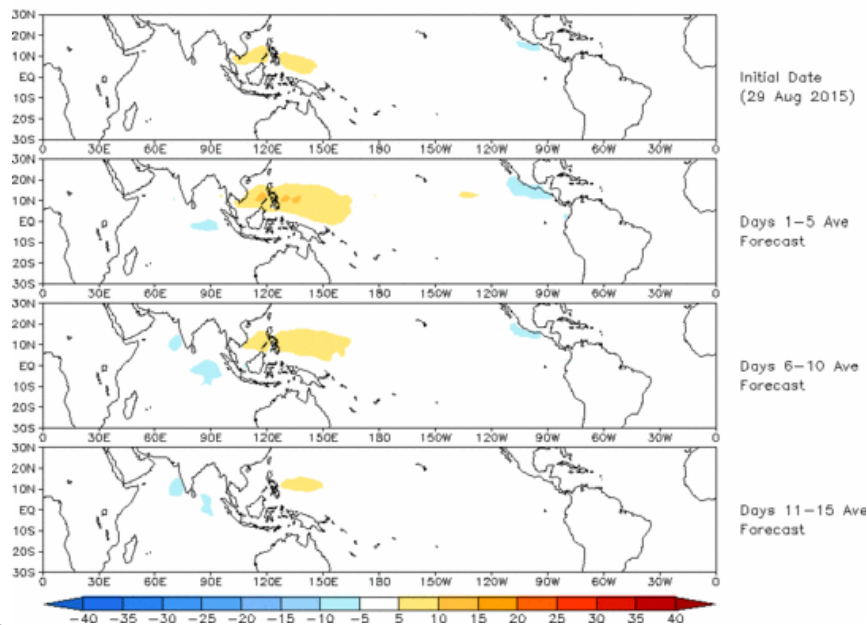
Reconstructed anomaly field associated with the MJO using RMM1 & RMM2
OLR [7.5°S,7.5°N] (cint:4Wm²) Period:27-Feb-2015 to 29-Aug-2015
The unfilled contours are GEFS forecast reconstructed anomaly for 15 days



Constructed Analog (CA) MJO Forecast

Spatial map of OLR anomalies for the next 15 days

OLR prediction of MJO-related anomalies using CA model
reconstruction by RMM1 & RMM2 (29 Aug 2015)

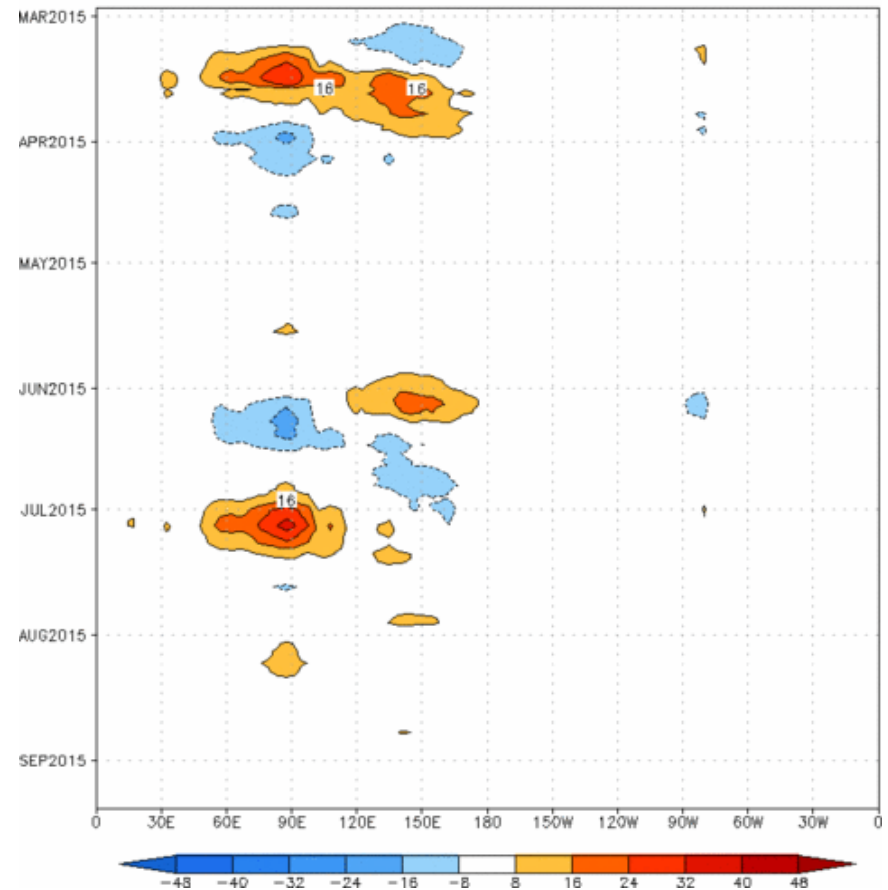


The constructed analog model also depicts a weak anomaly pattern.

Figures below show MJO associated OLR anomalies only (reconstructed from RMM1 and RMM2) and do not include contributions from other modes (*i.e.*, ENSO, monsoons, etc.)

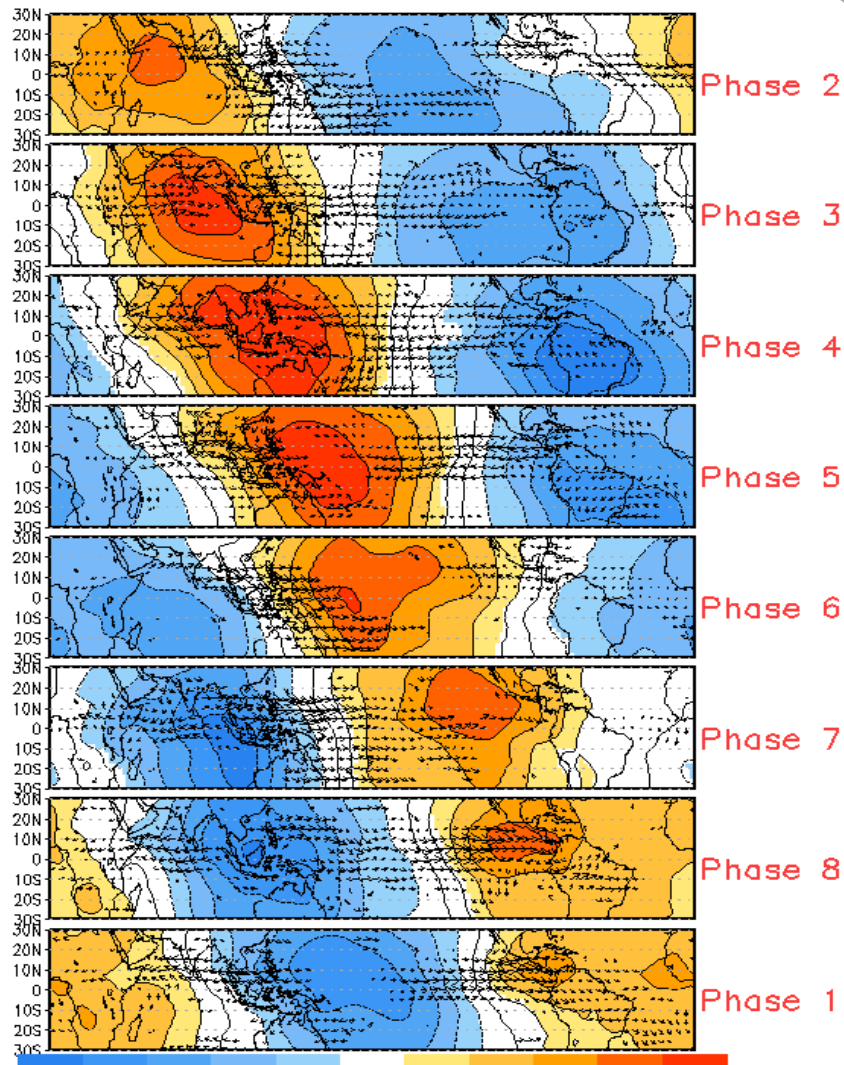
Time-longitude section of (7.5° S- 7.5° N) OLR anomalies - last 180 days and for the next 15 days

Reconstructed anomaly field associated with the MJO using RMM1 & RMM2
OLR [7.5° S, 7.5° N] ($\text{cint: } 4\text{Wm}^{-2}$) Period: 27-Feb-2015 to 29-Aug-2015
The unfilled contours are CA forecast reconstructed anomaly for 15 days

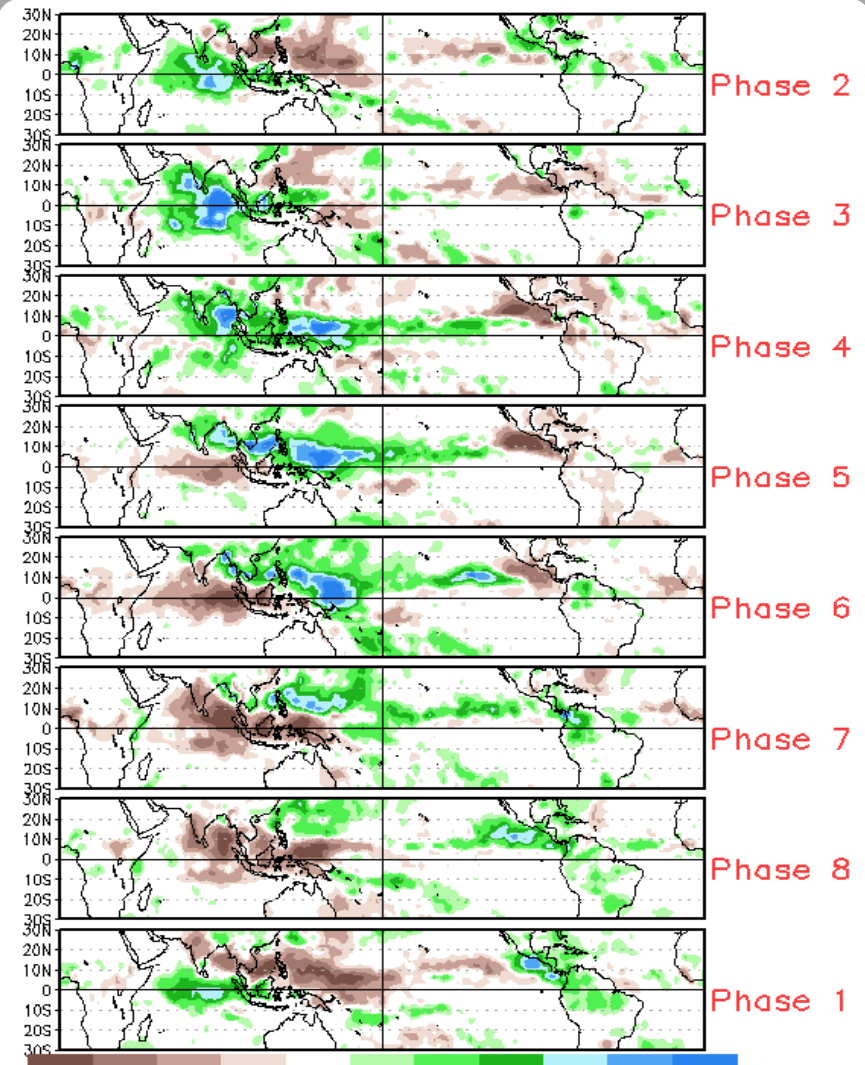


MJO Composites - Global Tropics

850-hPa Velocity Potential and
Wind Anomalies (May-Sep)



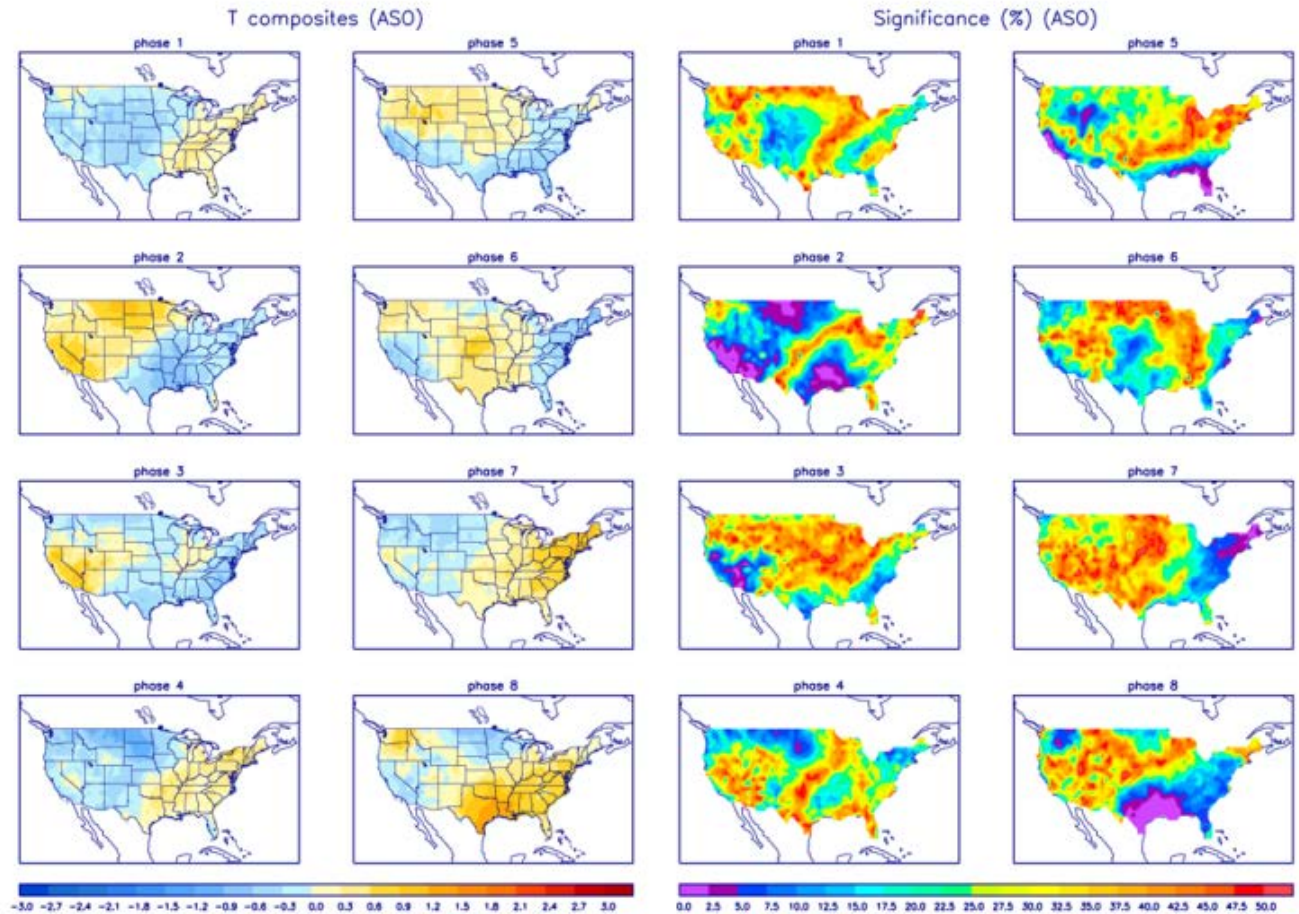
Precipitation Anomalies (May-Sep)



U.S. MJO Composites - Temperature

Left hand side plots show temperature anomalies by MJO phase for MJO events that have occurred over the three month period in the historical record. Blue (orange) shades show negative (positive) anomalies respectively.

Right hand side plots show a measure of significance for the left hand side anomalies. Purple shades indicate areas in which the anomalies are significant at the 95% or better confidence level.



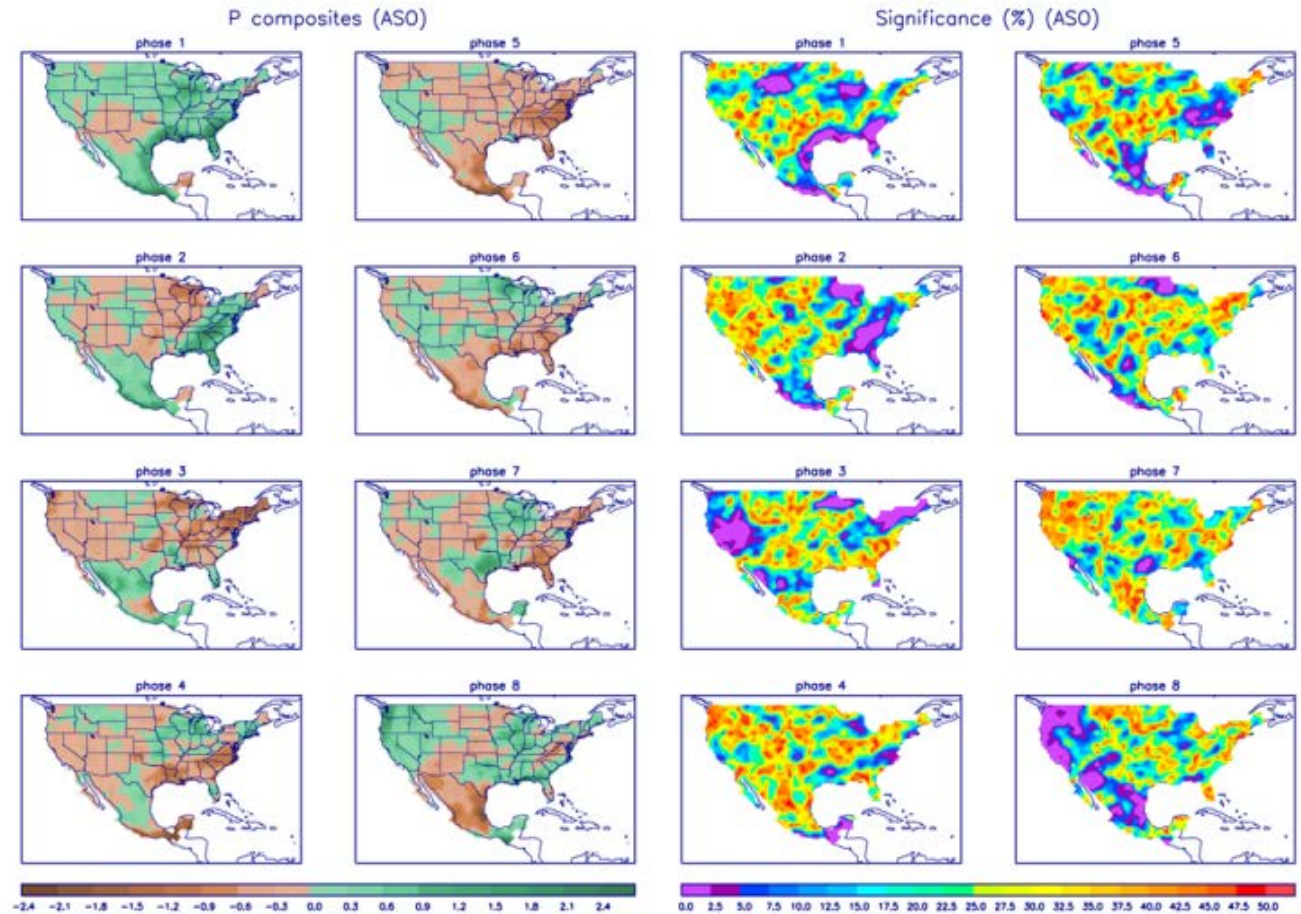
Zhou et al. (2011): A composite study of the MJO influence on the surface air temperature and precipitation over the Continental United States, *Climate Dynamics*, 1-13, doi: 10.1007/s00382-011-1001-9

<http://www.cpc.ncep.noaa.gov/products/precip/CWlink/MJO/mjo.shtml>

U.S. MJO Composites - Precipitation

Left hand side plots show precipitation anomalies by MJO phase for MJO events that have occurred over the three month period in the historical record. Brown (green) shades show negative (positive) anomalies respectively.

Right hand side plots show a measure of significance for the left hand side anomalies. Purple shades indicate areas in which the anomalies are significant at the 95% or better confidence level.



Zhou et al. (2011): A composite study of the MJO influence on the surface air temperature and precipitation over the Continental United States, *Climate Dynamics*, 1-13, doi: 10.1007/s00382-011-1001-9

<http://www.cpc.ncep.noaa.gov/products/precip/CWlink/MJO/mjo.shtml>